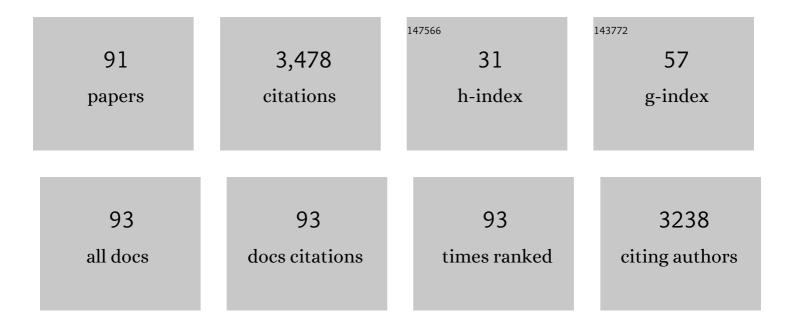
Hein WJP Neomagus

List of Publications by Year in descending order

Source: https://exaly.com/author-pdf/6551106/publications.pdf Version: 2024-02-01



HEIN WIP NEOMACUS

#	Article	IF	CITATIONS
1	Co-pyrolysis of torrefied biomass and coal: Effect of pressure on synergistic reactions. Journal of Analytical and Applied Pyrolysis, 2022, 161, 105363.	2.6	15
2	Lumped chemical kinetic modelling of raw and torrefied biomass under pressurized pyrolysis. Energy Conversion and Management, 2022, 253, 115199.	4.4	8
3	The influence of particle size on the thermal performance of coal and its derived char in a Union stove. Energy Geoscience, 2021, 2, 148-159.	1.3	9
4	Co-pyrolysis of coal and raw/torrefied biomass: A review on chemistry, kinetics and implementation. Renewable and Sustainable Energy Reviews, 2021, 135, 110189.	8.2	101
5	Effect of the V5+ to V4+ Molar Ratio on H2S Absorption and Conversion to Elemental Sulfur. Industrial & Engineering Chemistry Research, 2021, 60, 1505-1516.	1.8	1
6	Recent Advances in Membrane-Based Electrochemical Hydrogen Separation: A Review. Membranes, 2021, 11, 127.	1.4	39
7	Hydrogen Separation and Purification from Various Gas Mixtures by Means of Electrochemical Membrane Technology in the Temperature Range 100–160 °C. Membranes, 2021, 11, 282.	1.4	32
8	An experimentally validated computational model to predict the performance of a single-channel laboratory-scale electrostatic precipitator equipped with spiked and wire discharge electrodes. Journal of Electrostatics, 2021, 112, 103595.	1.0	10
9	The CO Tolerance of Pt/C and Pt-Ru/C Electrocatalysts in a High-Temperature Electrochemical Cell Used for Hydrogen Separation. Membranes, 2021, 11, 670.	1.4	2
10	Coal reactivity and selection for solid-based pre-reduction of sponge iron. International Journal of Coal Preparation and Utilization, 2020, 40, 233-246.	1.2	2
11	The effect of particle size on the pollution reduction potential of a South African coal-derived low-smoke fuel. Energy Geoscience, 2020, 1, 165-173.	1.3	3
12	Significance of coal properties on the caking degree of coarse coal particles mined at Limpopo Province, Republic of South Africa. International Journal of Coal Preparation and Utilization, 2020, 40, 297-319.	1.2	2
13	Dataset on the carbon dioxide, methane and nitrogen high-pressure sorption properties of South African bituminous coals. Data in Brief, 2019, 25, 104248.	0.5	4
14	Mineralogy and Petrology of Chars Produced by South African Caking Coals and Density-Separated Fractions during Pyrolysis and Their Effects on Caking Propensity. Energy & Fuels, 2019, 33, 7645-7658.	2.5	14
15	The carbon dioxide, methane and nitrogen high-pressure sorption properties of South African bituminous coals. International Journal of Coal Geology, 2019, 209, 40-53.	1.9	22
16	Transformation of nitrogen functional forms and the accompanying chemical-structural properties emanating from pyrolysis of bituminous coals. Applied Energy, 2018, 216, 414-427.	5.1	34
17	The carbon dioxide gasification characteristics of biomass char samples and their effect on coal gasification reactivity during co-gasification. Bioresource Technology, 2018, 258, 70-78.	4.8	83
18	Release of Nitrogenous Volatile Species from South African Bituminous Coals during Pyrolysis. Energy & Fuels, 2018, 32, 4606-4616.	2.5	14

HEIN W J P NEOMAGUS

#	Article	IF	CITATIONS
19	The influence of design parameters on the occurrence of shielding in multi-electrode ESPs and its effect on performance. Journal of Electrostatics, 2018, 93, 17-30.	1.0	19
20	The effect of carbon dioxide partial pressure on the gasification rate and pore development of Highveld coal chars at elevated pressures. Fuel Processing Technology, 2018, 179, 1-9.	3.7	12
21	Manufacturing and testing of briquettes from inertinite-rich low-grade coal fines using various binders. Journal of the South African Institute of Mining and Metallurgy, 2018, 118, 83-88.	0.5	9
22	Influence of additives on the devolatilization product yield of typical South African coals, and effect on tar composition. Journal of the Southern African Institute of Mining and Metallurgy, 2018, 118, 395-407.	0.1	3
23	Transport properties of chitosan membranes for zinc (II) removal from aqueous systems. Separation and Purification Technology, 2017, 179, 428-437.	3.9	18
24	Coal-derived low smoke fuel assessment through coal stove combustion testing. Journal of Analytical and Applied Pyrolysis, 2017, 126, 158-168.	2.6	11
25	The effect of acid demineralising bituminous coals and de-ashing the respective chars on nitrogen functional forms. Journal of Analytical and Applied Pyrolysis, 2017, 125, 127-135.	2.6	35
26	Evaluation and prediction of slow pyrolysis products derived from coals of different rank. Journal of Analytical and Applied Pyrolysis, 2017, 128, 156-167.	2.6	30
27	Chemical and structural characterization of char development during lignocellulosic biomass pyrolysis. Bioresource Technology, 2017, 243, 941-948.	4.8	38
28	Particle size influence on the pore development of nanopores in coal gasification chars: From micron to millimeter particles. Carbon, 2017, 112, 37-46.	5.4	32
29	Experimentation and CFD modelling of a microchannel reactor for carbon dioxide methanation. Chemical Engineering Journal, 2017, 313, 847-857.	6.6	57
30	Effect of Relative Humidity and Temperature on the Mechanical Properties of PFSA Nafionâ,,¢-cation-exchanged membranes for Electrochemical Applications. International Journal of Electrochemical Science, 2017, 12, 2573-2582.	0.5	5
31	The effect of added minerals on the pyrolysis products derived from a vitrinite-rich demineralised South African coal. Journal of Analytical and Applied Pyrolysis, 2016, 121, 41-49.	2.6	21
32	CFD modeling of particle charging and collection in electrostatic precipitators. Journal of Electrostatics, 2016, 84, 10-22.	1.0	60
33	Hydrogen production from ammonia decomposition over a commercial Ru/Al2O3 catalyst in a microchannel reactor: Experimental validation and CFD simulation. International Journal of Hydrogen Energy, 2016, 41, 3774-3785.	3.8	48
34	Structural and chemical modifications of typical South African biomasses during torrefaction. Bioresource Technology, 2016, 202, 192-197.	4.8	59
35	The properties of large coal particles and reaction kinetics of corresponding chars. Fuel, 2015, 140, 17-26.	3.4	9
36	The effect of acid washing on the pyrolysis products derived from a vitrinite-rich bituminous coal. Journal of Analytical and Applied Pyrolysis, 2015, 116, 142-151.	2.6	28

HEIN WJP NEOMAGUS

#	Article	IF	CITATIONS
37	Sulphur trioxide decomposition with supported platinum/palladium on rutile catalyst: 2. Performance of a laboratory fixed bed reactor. International Journal of Hydrogen Energy, 2015, 40, 2493-2499.	3.8	7
38	Performance evaluation of a high-throughput microchannel reactor for ammonia decomposition over a commercial Ru-based catalyst. International Journal of Hydrogen Energy, 2015, 40, 2921-2926.	3.8	33
39	Chemical–structural properties of South African bituminous coals: Insights from wide angle XRD–carbon fraction analysis, ATR–FTIR, solid state 13 C NMR, and HRTEM techniques. Fuel, 2015, 158, 779-792.	3.4	262
40	Reactivity study of fine discard coal agglomerates. Journal of Analytical and Applied Pyrolysis, 2015, 113, 723-728.	2.6	5
41	Reduction of Caking Propensity in Large (Millimeter-Sized) South African Coal Particles with Potassium Carbonate Impregnation To Expand Fixed- and Fluidized-Bed Gasification Feedstock Suitability. Energy & Fuels, 2015, 29, 4255-4263.	2.5	2
42	Density functional theory molecular modelling and experimental particle kinetics for CO2–char gasification. Carbon, 2015, 93, 295-314.	5.4	58
43	Leaching kinetics of bottom ash waste as a source of calcium ions. Journal of the Air and Waste Management Association, 2015, 65, 126-132.	0.9	4
44	Effect of Fly Ash as an Additive on the Limestone Dissolution Rate Constant. Energy & Fuels, 2015, 29, 3284-3291.	2.5	2
45	The characterisation of slow-heated inertinite- and vitrinite-rich coals from the South African coalfields. Fuel, 2015, 158, 591-601.	3.4	36
46	Pore development during gasification of South African inertinite-rich chars evaluated using small angle X-ray scattering. Carbon, 2015, 95, 250-260.	5.4	32
47	Influence of Potassium Carbonate on the Swelling Propensity of South African Large Coal Particles. Energy & Fuels, 2015, 29, 6197-6205.	2.5	3
48	A laboratory scale fixed-bed coal conversion reactor part 1: Operation, reaction zone identification and industrial representativeness. Journal of Analytical and Applied Pyrolysis, 2015, 115, 428-436.	2.6	3
49	Sulphur trioxide decomposition with supported platinum/palladium on rutile catalysts: 1. Reaction kinetics of catalyst pellets. International Journal of Hydrogen Energy, 2015, 40, 85-94.	3.8	11
50	Comparing the porosity and surface areas of coal as measured by gas adsorption, mercury intrusion and SAXS techniques. Fuel, 2015, 141, 293-304.	3.4	360
51	Influence of maceral composition on the structure, properties and behaviour of chars derived from South African coals. Fuel, 2015, 142, 9-20.	3.4	89
52	A perspective on South African coal fired power station emissions. Journal of Energy in Southern Africa, 2015, 26, 27-40.	0.5	26
53	Dissolution kinetics of South African coal fly ash and the development of a semi-empirical model to predict dissolution. Chemical Industry and Chemical Engineering Quarterly, 2015, 21, 319-330.	0.4	6
54	Dissolution kinetics of sorbents and effect of additives in wet flue gas desulfurization. Reviews in Chemical Engineering, 2014, 30, .	2.3	9

HEIN WJP NEOMAGUS

#	Article	IF	CITATIONS
55	Experimental performance evaluation of an ammonia-fuelled microchannel reformer for hydrogen generation. International Journal of Hydrogen Energy, 2014, 39, 7225-7235.	3.8	17
56	SO ₂ Solubility in 50 wt % H ₂ SO ₄ at Elevated Temperatures and Pressures. Journal of Chemical & Engineering Data, 2014, 59, 1-7.	1.0	12
57	The transient swelling behaviour of large (â^'20 + 16 mm) South African coal particles during low-temperature devolatilisation. Fuel, 2014, 136, 79-88.	3.4	48
58	Modeling the Nonisothermal Devolatilization Kinetics of Typical South African Coals. Energy & Fuels, 2014, 28, 920-933.	2.5	12
59	An evaluation of a new automated duplicate-sample Fischer Assay setup according to ISO/ASTM standards and analysis of the tar fraction. Journal of Analytical and Applied Pyrolysis, 2014, 106, 190-196.	2.6	17
60	A modelling evaluation of an ammonia-fuelled microchannel reformer for hydrogen generation. International Journal of Hydrogen Energy, 2014, 39, 11390-11402.	3.8	38
61	Semiâ€Empirical Model for Limestone Dissolution in Adipic Acid for Wet Flue Gas Desulfurization. Chemical Engineering and Technology, 2014, 37, 1919-1928.	0.9	0
62	The use of thermomechanical analysis to characterise Söderberg electrode paste raw materials. Minerals Engineering, 2013, 46-47, 167-176.	1.8	8
63	Reactor technology options for distributed hydrogen generation via ammonia decomposition: A review. International Journal of Hydrogen Energy, 2013, 38, 14968-14991.	3.8	131
64	A Comparative Study of the Processing Scheme of Chitosan and Nafion 117 in Membrane Electrode Assembly. Petroleum Science and Technology, 2013, 31, 121-128.	0.7	0
65	Improved reactivity of large coal particles by K2CO3 addition during steam gasification. Fuel Processing Technology, 2013, 114, 75-80.	3.7	52
66	X-ray diffraction parameters and reaction rate modeling for gasification and combustion of chars derived from inertinite-rich coals. Fuel, 2013, 109, 148-156.	3.4	67
67	Elucidation of the Structural and Molecular Properties of Typical South African Coals. Energy & Fuels, 2013, 27, 3161-3172.	2.5	31
68	Influence of Chemical Pretreatment on the Internal Structure and Reactivity of Pyrolysis Chars Produced from Sugar Cane Bagasse. Energy & Fuels, 2012, 26, 4497-4506.	2.5	24
69	The random pore model with intraparticle diffusion for the description of combustion of char particles derived from mineral- and inertinite rich coal. Fuel, 2011, 90, 2347-2352.	3.4	30
70	Assessing the catalytic effect of coal ash constituents on the CO2 gasification rate of high ash, South African coal. Fuel Processing Technology, 2011, 92, 2048-2054.	3.7	87
71	Thermal reduction of barium sulphate with carbon monoxide—A thermogravimetric study. Thermochimica Acta, 2010, 498, 67-70.	1.2	9
72	The adsorption of copper in a packed-bed of chitosan beads: Modeling, multiple adsorption and regeneration. Journal of Hazardous Materials, 2009, 167, 1242-1245.	6.5	40

HEIN WJP NEOMAGUS

#	Article	IF	CITATIONS
73	A kinetic expression for the pyrolytic decomposition of polytetrafluoroethylene. Journal of Fluorine Chemistry, 2008, 129, 314-318.	0.9	7
74	The influence of the degree of cross-linking on the adsorption properties of chitosan beads. Bioresource Technology, 2008, 99, 7377-7382.	4.8	93
75	Properties of high ash char particles derived from inertinite-rich coal: 1. Chemical, structural and petrographic characteristics. Fuel, 2008, 87, 3082-3090.	3.4	42
76	Properties of high ash coal-char particles derived from inertinite-rich coal: II. Gasification kinetics with carbon dioxide. Fuel, 2008, 87, 3403-3408.	3.4	85
77	Kinetic analysis of non-isothermal thermogravimetric analyser results using a new method for the evaluation of the temperature integral and multi-heating rates. Fuel, 2006, 85, 418-422.	3.4	25
78	Reaction kinetics of pulverized coal-chars derived from inertinite-rich coal discards: Gasification with carbon dioxide and steam. Fuel, 2006, 85, 1076-1082.	3.4	168
79	Reaction kinetics of pulverized coal-chars derived from inertinite-rich coal discards: Characterisation and combustion. Fuel, 2006, 85, 1067-1075.	3.4	26
80	A comparison of glycans and polyglycans using solid-state NMR and X-ray powder diffraction. Solid State Nuclear Magnetic Resonance, 2006, 30, 150-161.	1.5	20
81	The modeling of the combustion of high-ash coal–char particles suitable for pressurised fluidized bed combustion: shrinking reacted core model. Fuel, 2005, 84, 1136-1143.	3.4	13
82	Salt rejection in nanofiltration for single and binary salt mixtures in view of sulphate removal. Desalination, 2005, 171, 205-215.	4.0	86
83	Organicâ€Organic Separation by Pervaporation. II. Separation of Methanol from Tame by an αâ€Alumina Supported Nayâ€Zeolite Membrane. Separation Science and Technology, 2005, 40, 1047-1065.	1.3	4
84	A Predictive Model for Permeation Flux in a Membrane Reactor: Aspects of Esterification. Separation Science and Technology, 2005, 40, 433-452.	1.3	2
85	Copper(II) removal from polluted water with alumina/chitosan composite membranes. Journal of Membrane Science, 2002, 197, 147-156.	4.1	108
86	Pervaporation separation of methanol from methanol/tert-amyl methyl ether mixtures with a commercial membrane. Journal of Membrane Science, 2002, 209, 353-362.	4.1	26
87	Centrifugal casting of ceramic membrane tubes and the coating with chitosan. Separation and Purification Technology, 2001, 25, 407-413.	3.9	33
88	A FIXED BED BARRIER REACTOR WITH SEPARATE FEED OF REACTANTS. Chemical Engineering Communications, 2001, 184, 49-69.	1.5	3
89	The catalytic combustion of natural gas in a membrane reactor with separate feed of reactants. Chemical Engineering Journal, 2000, 77, 165-177.	6.6	30
90	High-temperature membrane reactors: potential and problems. Chemical Engineering Science, 1999, 54, 1997-2017.	1.9	230

#	Article	IF	CITATIONS
91	The catalytic oxidation of H2S in a stainless steel membrane reactor with separate feed of reactants. Journal of Membrane Science, 1998, 148, 147-160.	4.1	16